[5] A. J. Weiss and B. Friedlander, "Performance analysis of diversly polarized antenna arrays," *IEEE Trans. Signal Process.*, vol. 39, pp. 1589–1603, July 1991.
[6] Y. Hua and T. K. Sarkar, "Generalized pencil-of-functions method for extracting the poles of an electromagnetic system from its transient response," *IEEE Trans. Antennas Propagat.*, vol. 37, pp. 229–234, Feb. 1989.
[7] Y. Hua and T. K. Sarkar, "Matrix pencil method for estimating parameters of exponentially damped/undamped sinusoids in noise," *IEEE Trans. Acoust., Speech, Signal Process.*, vol. 38, pp. 814–824, May 1990.
[8] Y. Hua, "Estimating two-dimensional frequencies by matrix enhancement and matrix pencil," in *Proc. IEEE ICASSP91* (Toronto, Canada), May 1991.
[9] R. O. Schmidt, "A signal subspace approach to multiple emitter location and spectral estimation," Ph.D. dissertation, Stanford University, CA, 1981.
[10] R. H. Roy, "ESPRIT—Estimation of signal parameters via rotational invariance techniques," Ph.D. dissertation, Stanford University, CA, 1987.
[11] T. J. Shan, M. Wax, and T. Kailath, "On spatial smoothing for direction-of-arrival estimation of coherent signals," *IEEE Trans. Acoust., Speech, Signal Process.*, vol. 33, pp. 806–811, Aug. 1985.
[12] W. Chen, K. M. Wong, and J. P. Reilly, "Detection of the number of signals: a predicted eigen-threshold approach," *IEEE Trans. Signal Process.*, vol. 39, pp. 1088–1098, May 1991.
[13] Y. Hua and T. K. Sarkar, "On SVD for estimating generalized eigenvalues of matrix pencil in noise," *IEEE Trans. Signal Process.*, vol. 39, pp. 892–900, Apr. 1991.
[14] H. L. Van Trees, *Detection, Estimation and Modulation Theory, Part I.* New York: Wiley, 1968.
[15] R. Kumaresan and D. W. Tufts, "Estimating the angles of arrival of multiple plane waves," *IEEE Trans. Aerospace Electron. Syst.*, vol. 19, pp. 134–139, Jan. 1983.

The RCS of a Microstrip Dipole Deduced from an Expansion of Pole Singularities

George W. Hanson and Dennis P. Nyquist

Abstract—**The singularity expansion method (SEM) is applied to the steady-state analysis of plane wave scattering from microstrip dipoles. The current induced on the antenna is expanded in a series of natural modes, where the amplitude of each term in the expansion is expressed as a coupling coefficient weighted by a simple frequency pole. Natural modes occur at pole singularities of the antenna current in the complex frequency plane, and are found by a numerical root search of a homogeneous matrix equation. This formulation results in an accurate and efficient calculation of the radar cross section (RCS) of microstrip dipoles which exhibit some appreciable resonant characteristics, where it is found that the current resonance dominates the response of the antenna. The SEM applied here yields good physical insight into the scattering behavior of such antennas. Results obtained with the SEM analysis are compared with a full-wave method of moments (MoM) solution.**

I. Introduction

Microstrip antennas frequently find application on vehicles since they are lightweight, conformal, and relatively inexpensive. Because they are often found on the exterior of vehicles, determination of their RCS is important. While the radiation and input properties of microstrip dipoles have been studied extensively, their scattering properties have only recently been addressed [1], although scattering from microstrip patch antennas has been considered by several authors [2]–[4].

Manuscript received April 24, 1992; revised November 2, 1992.

G. W. Hanson is with the Department of Electrical Engineering and Computer Science, University of Wisconsin-Milwaukee, Milwaukee, WI 53201.
D. P. Nyquist is with the Department of Electrical Engineering, Michigan State University, East Lansing, MI 48824.

IEEE Log Number 9207125.

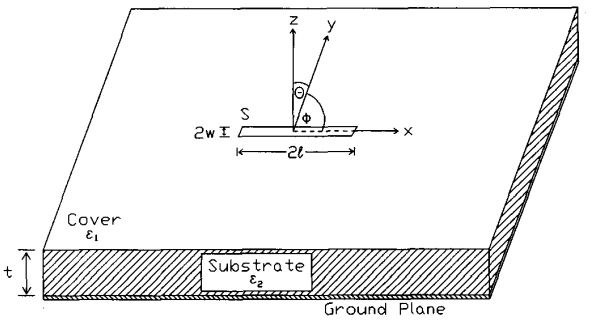

Fig. 1. Microstrip dipole geometry.

In this work, the RCS of a microstrip dipole based upon a pole-singularity expansion (PSE) of the antenna current is presented. The current expansion is formed as a series of natural modes, where a "natural mode" refers to a complex resonant frequency and the associated current distribution. The amplitude of each term in the series is given by a coupling coefficient weighted by a simple frequency pole. The coupling coefficients, which are overlap integrals between the natural modes of the antenna and the incident excitation, are similar in form to the "class 1" coupling coefficients used in the well-known singularity expansion method (SEM) [5]–[7], although their evaluation is complicated by the presence of the Green function for the microstrip environment.

The RCS of several microstrip dipole configurations is presented, and results are compared with a full-wave MoM solution. The efficiency and accuracy of this method, as well as the range of its applicability, are discussed. It is found that the PSE method provides good physical insight into the dominant scattering phenomena for dipoles printed on generally lossy thin substrates.

II. Theory

The geometry of a microstrip dipole is shown in Fig. 1. The dielectric cover and substrate, regions 1 and 2, respectively, are assumed to be linear, isotropic, and homogeneous, with relative permitivity ϵ_{ri} and loss tangent $\tan\delta_i$ for the ith region. The wave number and intrinsic impedance in each region are $k_i = \sqrt{\epsilon_i}k_0$ and $\eta_i = \eta_0/\sqrt{\epsilon_i}$, where (k_0, η_0) are their free-space counterparts. For the results presented here the cover region is assumed to be free space, and the substrate is nonmagnetic.

The electric field in the cover maintained by currents in the cover is

$$\vec{E}_1(\vec{r}) = \frac{-j\eta_1}{k_1}\int_S \overleftrightarrow{G}^e(\vec{r} \mid \vec{r}') \cdot \vec{K}(\vec{r}')\, dS', \qquad (1)$$

where $\overleftrightarrow{G}^e(\vec{r} \mid \vec{r}')$ is an appropriate electric dyadic Green function for the layered geometry [8]. Scattering from a microstrip dipole is deduced from the EFIE

$$-\frac{j\eta_1}{k_1}\hat{t} \cdot \int_S \overleftrightarrow{G}^e(\vec{r} \mid \vec{r}') \cdot \vec{K}(\vec{r}')\, dS' = -\hat{t} \cdot \vec{E}_1^i(\vec{r}) \ldots \forall \vec{r} \in S, \quad (2)$$

obtained by enforcing the tangential boundary condition for the electric field at the perfectly conducting dipole surface S. The field $\vec{E}_1^i$ is the impressed excitation and $\hat{t}$ is a unit vector tangent to the perfectly conducting dipole.

A. Singularity Expansion Formulation

The current in (2) is expanded in a series of pole singularities [9], [10]:

$$\vec{K}(\vec{r}, \omega) \approx \sum_{q=1}^{Q} \frac{A_q \vec{k}_q(\vec{r})}{(\omega - \omega_q)}, \tag{3}$$

where ω_q is a complex natural frequency, $\vec{k}_q$ is the natural-mode current distribution associated with the qth natural mode, and A_q is the corresponding amplitude coefficient. The pth natural mode satisfies the homogeneous EFIE

$$\hat{t} \cdot \int_S \overleftrightarrow{G}^e(\vec{r} \mid \vec{r}'; \omega) \cdot \vec{k}_p(\vec{r}')\, dS' = 0 \ldots \forall \vec{r} \in S \tag{4}$$

with nontrivial solutions only for $\omega = \omega_p$.

The excitation amplitude for natural-mode current, A_q, relates the amplitude of the qth natural mode to the impressed excitation. These amplitudes are determined from the fundamental EFIE (2) and current expansion (3) upon invoking reciprocity of the Green dyad kernel, $G_{\alpha\beta}(\vec{r} \mid \vec{r}') = G_{\beta\alpha}(\vec{r}' \mid \vec{r})$. The derivation of A_q, which is referred to as a coupling coefficient in the SEM literature [7], is summarized as follows.

The integral operator $\int_S dS\, \vec{k}_p(\vec{r}) \cdot \{\cdots\}$, which performs the $\hat{t} \cdot \{\cdots\}$ operation, is applied to EFIE (2), yielding

$$\int_S dS'\, \vec{K}(\vec{r}') \cdot \int_S \overleftrightarrow{G}^e(\vec{r}' \mid \vec{r}; \omega) \cdot \vec{k}_p(\vec{r})\, dS = -\frac{jk_1}{\eta_1} \int_S \vec{k}_p(\vec{r}) \cdot \vec{E}_1^i(\vec{r})\, dS,$$

where reciprocity of the Green dyad has been invoked. Since dominant interactions are expected for $\omega \approx \omega_p$, $\overleftrightarrow{G}^e(\vec{r} \mid \vec{r}'; \omega)$ is expanded in a Taylor's series about $\omega = \omega_p$, leading to

$$\int_S dS'\, \vec{K}(\vec{r}') \cdot \int_S \left[\overleftrightarrow{G}^e(\vec{r}' \mid \vec{r}, \omega_p) + \left.\frac{\partial \overleftrightarrow{G}^e(\vec{r}' \mid \vec{r}, \omega)}{\partial \omega}\right|_{\omega=\omega_p} (\omega - \omega_p) + \cdots\right] \cdot \vec{k}_p(\vec{r})\, dS = -\frac{jk_1}{\eta_1} \int_S \vec{k}_p(\vec{r}) \cdot \vec{E}_1^i(\vec{r})\, dS.$$

The leading term vanishes because of (4); consequently

$$\int_S dS'\, \vec{K}(\vec{r}') \cdot \int_S \left[\left.\frac{\partial \overleftrightarrow{G}^e(\vec{r}' \mid \vec{r}; \omega)}{\partial \omega}\right|_{\omega=\omega_p} (\omega - \omega_p) + \cdots\right] \cdot \vec{k}_p(\vec{r})\, dS = -\frac{jk_1}{\eta_1} \int_S \vec{k}_p(\vec{r}) \cdot \vec{E}_1^i(\vec{r})\, dS.$$

Singularity expansion (3) is exploited in the above, leading to

$$\sum_q \frac{A_q}{(\omega - \omega_q)} \int_S dS'\, \vec{k}_q(\vec{r}') \cdot \int_S \left[\left.\frac{\partial \overleftrightarrow{G}^e(\vec{r}' \mid \vec{r}; \omega)}{\partial \omega}\right|_{\omega=\omega_p} (\omega - \omega_p) + \cdots\right] \cdot \vec{k}_p(\vec{r})\, dS = -\frac{jk_1}{\eta_1} \int_S \vec{k}_p(\vec{r}) \cdot \vec{E}_1^i(\vec{r}, \omega)\, dS.$$

In the limit $\omega \to \omega_p$ only the $q = p$ term is nonvanishing, resulting in the coupling coefficient

$$A_p = \lim_{\omega \to \omega_p} -\frac{jk_1}{\eta_1 C_p} \int_S \vec{k}_p(\vec{r}) \cdot \vec{E}_1^i(\vec{r}, \omega)\, dS, \tag{5}$$

where natural-mode currents are normalized such that (reciprocity invoked again)

$$C_p = \int_S dS\, \vec{k}_p(\vec{r}) \cdot \int_S \left.\frac{\partial \overleftrightarrow{G}^e(\vec{r} \mid \vec{r}'; \omega)}{\partial \omega}\right|_{\omega=\omega_p} \cdot \vec{k}_p(\vec{r}')\, dS'. \tag{6}$$

The coupling coefficients (5) quantify the amplitude of resonant antenna currents induced by fields maintained by currents elsewhere in the system. If $\vec{E}_1^i$ maintained by impressed current $\vec{J}^i$ is expressed as a volume integral in the form of (1), and reciprocity of the Green dyad is invoked, coupling coefficient A_p becomes

$$A_p = \lim_{\omega \to \omega_p} -\frac{1}{C_p} \int_V dV'\, \vec{J}^i(\vec{r}') \cdot \int_S \overleftrightarrow{G}^e(\vec{r}' \mid \vec{r}; \omega) \cdot \vec{k}_p(\vec{r})\, dS. \tag{7}$$

The inner integral is seen to be proportional to the natural-mode field in the cover,

$$\vec{E}_1^p(\vec{r}) = \frac{-j\eta_1}{k_1} \int_S \overleftrightarrow{G}^e(\vec{r} \mid \vec{r}') \cdot \vec{k}_p(\vec{r}')\, dS', \tag{8}$$

leading to the coupling coefficient

$$A_p = \lim_{\omega \to \omega_p} -\frac{jk_1}{\eta_1 C_p} \int_V \vec{J}^i(\vec{r}) \cdot \vec{E}_1^p(\vec{r}, \omega)\, dV. \tag{9}$$

If the incoming plane wave is polarized in the $\hat{\alpha}$ direction, an equivalent dipole source in the cover layer at (r_1, θ_1, ϕ_1) which produces this unit amplitude wave is

$$\vec{J}_d^i = \hat{\alpha}\left(\frac{j4\pi r_1}{\omega\mu_1}\right) \delta(\vec{r} - \vec{r}_1). \tag{10}$$

The coupling coefficient is then reduced to

$$A_p = \lim_{\omega \to \omega_p} \frac{4\pi r_1}{C_p \eta_1^2} \hat{\alpha} \cdot \vec{E}_1^p(r_1, \theta_1, \phi_1), \tag{11}$$

where $\vec{E}_1^p$ can be evaluated in closed form by the method of stationary phase since r_1 is assumed large for RCS applications.

Subsequent to identification of the natural current resonances and evaluation of coupling coefficients (11), the current induced on the antenna by the impressed excitation is completely determined. The field scattered by the antenna is found from (1) as a sum of appropriately weighted natural-mode fields:

$$\vec{E}_1^S(\vec{r}, \omega) = \sum_{q=1}^{Q} \frac{A_q \vec{E}_1^q(\vec{r})}{(\omega - \omega_q)}. \tag{12}$$

The radar cross section is computed as

$$\sigma_{\alpha\beta} = 4\pi r^2 |E_{1,\beta}^S|^2, \tag{13}$$

assuming that the incident plane wave is polarized in the $\hat{\alpha}$ direction and has unit amplitude.

B. Determination of Natural Modes

Singularity expansion (3) is expressed in terms of the natural modes of the microstrip dipole, obtained from (4) by a full-wave MoM/Galerkin solution. The current is expanded in a set of entire-domain basis functions,

$$\vec{k}_p(x, y) = \sum_{n=1}^{N} a_{pn} \vec{B}_n(x, y), \tag{14}$$

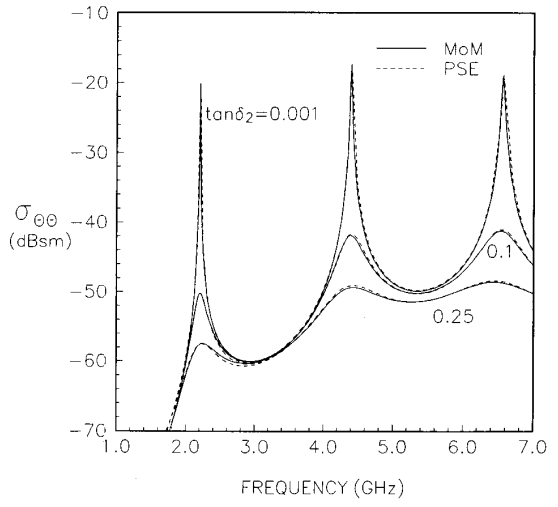

Fig. 2. Comparison of the RCS versus frequency for a microstrip dipole evaluated by the PSE and MoM methods. $\epsilon_{r2} = 2.2$, $l = 2.5$ cm, $w = 0.08$ cm, $\theta = 60°$, $\phi = 0°$, $t = 0.15$ cm, tan δ_2 varies.

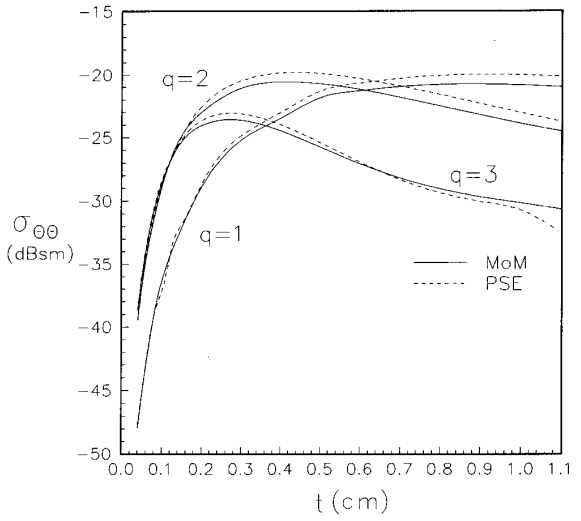

Fig. 3. RCS of a microstrip dipole evaluated at the first three resonant frequencies ($q = 1, 2, 3$) as the substrate thickness is varied. $\epsilon_{r2} = 2.2$, tan $\delta_2 = 0.01$, $l = 2.5$ cm, $w = 0.08$ cm, $\theta = 60°$, $\phi = 0°$.

with

$$\vec{B}_n(x, y) = \hat{x}\frac{\sin\left[\frac{n\pi}{2l}(x+l)\right]}{\sqrt{1-\left(\frac{y}{w}\right)^2}} \tag{15}$$

chosen to approximate the natural mode current distribution. Since (15) models the fundamental resonances of the antenna, convergence of the MoM solution is expected to be relatively rapid. Numerically this was found to be true, and typically a single term of (14) yields accurate results. Testing with the same function results in a matrix equation for the pth natural mode:

$$[Z_{mn}(\omega)][a_{pn}] = 0, \tag{16}$$

where

$$Z_{mn} = -\int_S \vec{B}_m \cdot \vec{E}_{1n}\, dS = Z_{nm} \tag{17}$$

and $\vec{E}_{1n}$ is the field in the cover caused by the nth basis function. The complex resonant frequency $\omega = \omega_p$ is found by a numerical root-search.

III. Results

A full-wave, entire-domain basis function Galerkin solution of (2) was obtained to provide a comparison with the approximate PSE method. Basis functions (15) were used as both expansion and testing functions. To confirm the accuracy of the MoM solution, a comparison with previously published results [1] was performed for a variety of substrate thicknesses, polarizations, and excitation angles, and agreement was found to be very good.

The RCS of a microstrip dipole versus frequency for a 5.0 cm × 0.16 cm dipole printed on a substrate with $\epsilon_{r2} = 2.2$ is shown in Fig. 2. The excitation geometry is $\theta = 60°$, $\phi = 0°$, and the monostatic RCS, $\sigma_{\theta\theta}$, is shown as loss in the substrate varies for a substrate thickness of 0.15 cm. The frequency range extends over the first three resonant peaks, q_1–q_3 in (3), corresponding to alternating even and odd modes. It can be seen that the PSE method yields results that are in good agreement with the MoM solution.

It was found that for tan $\delta_2 > 0.5$, the RCS does not exhibit any resonant behavior, and the PSE solution differs from the MoM solution by several dB. The PSE method is accurate for dipoles which exhibit some appreciable resonance, although it is seen that the dipole need not have an overly high Q.

The variation of RCS with substrate thickness is shown in Fig. 3 for the dipole of Fig. 2 with tan $\delta_2 = 0.01$. The monostatic RCS, $\sigma_{\theta\theta}$, is shown as t varies. The RCS is evaluated at the first three resonant frequencies, f_{q1}–f_{q3}, with $\theta = 60°$, $\phi = 0°$. The fundamental mode, $q = 1$, is weakly excited for very thin substrates, since the dipole and its image support an antisymmetric current mode, with little radiation. As the substrate thickness increases, the RCS evaluated at the fundamental resonance becomes dominant. Although not shown here, it was found that for broadside incidence, the fundamental mode became dominant much more quickly than depicted in Fig. 3.

For the results shown here, four natural-mode terms were used in current expansion (3). Each resonant frequency was found by a root search of (16) using one expansion function. The solution for the natural modes was relatively unaffected by increasing the number of expansion terms.

IV. Discussion

The PSE method is found to be an accurate and computationally efficient method for determining the RCS of microstrip dipoles printed on thin, generally lossy substrates. In order to implement the PSE solution, the natural-mode frequency and current distribution corresponding to each resonance must be determined. This requires a numerical root search of (16), which typically converges in a few iterations. A single basis function solution provides sufficient accuracy since the current distribution exactly at resonance is desired, and so the computation time for each natural mode is relativity short. It is important to note that the natural mode frequencies are excitation independent, and the normalization constant for each natural mode is excitation and frequency independent. Subsequent to numerical calculation of the natural-mode frequencies and normalization constants, the RCS (13) is generated as a function of frequency in closed form for any polarization or excitation angle. To evaluate the RCS for several different excitations, only the complex resonant frequencies

and normalization constants need to be stored, i.e., two complex numbers per resonance. The same analysis via the MoM solution would require storage of the impedance matrix at many frequencies in the range of interest.

V. Summary

The singularity expansion method (SEM) is applied to the steady-state analysis of plane wave scattering from microstrip dipoles. The current induced on the antenna is expanded as a series of pole-singularity terms, where each pole singularity corresponds to a natural mode of the dipole. These natural modes occur at complex frequencies, and are found efficiently by a numerical root search of a homogeneous matrix equation. This formulation results in an accurate and efficient calculation of the radar cross section (RCS) of microstrip dipoles which exhibit some appreciable current resonance. The pole singularity expansion provides good physical insight into the scattering behavior of such dipoles, and results are presented which illustrate the accuracy of the method.

References

[1] G. E. Antilla and N. G. Alexopoulos, "Surface wave and related effects on the RCS of microstrip dipoles printed on magnetodielectric substrates," *IEEE Trans. Antennas Propagat.*, vol. 39, pp. 1707–1715, Dec. 1991.

[2] E. H. Newman and D. Forrai, "Scattering from a microstrip patch," *IEEE Trans. Antennas Propagat.*, vol. 35, pp. 245–251, Mar. 1987.

[3] D. M. Pozar, "Radiation and scattering from a microstrip patch on a uniaxial substrate," *IEEE Trans Antennas Propagat.*, vol. 35, pp. 613–621, June 1987.

[4] D. R. Jackson, "The RCS of a rectangular microstrip patch in a substrate–superstrate geometry," *IEEE Trans. Antennas Propagat.*, vol. 38, pp. 2–8, Jan. 1990.

[5] C. E. Baum, "The singularity expansion method," in *Transient Electromagnetic Fields*, L. B. Felson, Ed. New York: Springer-Verlag, 1976, pp. 128–177.

[6] C. E. Baum, "Emerging technology for transient and broad-band analysis and synthesis of antennas and scatterers," *Proc. IEEE*, vol. 64, pp. 1598–1616, Nov. 1976.

[7] C. E. Baum, "The singularity expansion method: Background and developments," *IEEE Ant. Prop. Society Newsletter*, pp. 15–23, Aug. 1986.

[8] J. S. Bagby and D. P. Nyquist, "Dyadic Green's functions for integrated electronic and optical circuits," *IEEE Trans. Microwave Theory Tech.*, vol. 35, pp. 206–210, Feb. 1987.

[9] D. P. Nyquist, "Deduction of EM phenomena in microstrip circuits from an integral-operator description of the system," in *Proc. URSI Triennial EM Theory Symp.* (Stockholm, Sweden), Aug. 1989, pp. 533–535.

[10] G. W. Hanson, "The singularity expansion method for integrated electronics," Ph.D. dissertation, Michigan State University, East Lansing, 1991.

Direction and Polarization Estimation Using Arrays with Small Loops and Short Dipoles

Jian Li

Abstract— **This paper shows that when polarization-sensitive arrays consisting of crossed small loops and short dipoles are used, one can eliminate the requirement in the ESPRIT algorithm that sensors must occur in matched pairs. The dipoles and loops are sensitive to the polarizations of incident electromagnetic plane waves. The dipoles are sensitive to the incident electric field components and the loops to magnetic field components of the incident waves. We exploit the invariance properties among the dipole and loop outputs of an arbitrary array of orthogonal loops and orthogonal dipoles to compute both the two-dimensional arrival angles and polarizations of incoming narrow-band signals. We also show that with dipoles and loops, vertical arrays are not necessary to obtain good direction estimates for signals from low angles.**

I. Introduction

Many array signal processing algorithms have been devised for estimating the directions of arrival (DOA) of multiple narrow-band plane waves from sensor array data. Compared with the angle estimation, however, polarization estimation of electromagnetic plane waves has attracted much less attention. Moreover, the advantages of different polarization-sensitive arrays may be further exploited.

The problem of estimating signal polarizations along with arrival angles has been discussed previously by several authors. Schmidt [1] used the difference in polarizations of signals to improve their angle estimates. Ferrara and Parks [2] considered how to incorporate signal polarizations in Capon's minimum variance estimator [3], in the adapted angular response spectrum of Borgiotti and Kaplan [4], and in the MUSIC spectrum of Schmidt [5], [1]. Ziskind and Wax [6] described the use of the simulated annealing technique of Kirkpatrick *et al.* [7] to find maximum likelihood estimates of signal polarizations and arrival angles. Weiss and Friedlander [8] derived Cramer–Rao bounds for angle and polarization estimates when incident signals are linearly polarized and array elements are diversely circularly polarized. Li and Compton [9] presented how to use the computationally efficient ESPRIT algorithm of Roy and Kailath [10] to compute angle and polarization estimates with an array of crossed dipoles. Finally, Nehorai and Paldi [11] examined the advantages of using sensors that measure both electric and magnetic field components by deriving Cramer–Rao bounds. None of the previous work, however, has recognized the advantages of measuring both the electric and magnetic field components with a polarization-sensitive array in the ESPRIT algorithm.

The purpose of this paper is to show that when polarization-sensitive arrays consisting of crossed small loops and short dipoles are used, one can eliminate the requirement in the ESPRIT algorithm that sensors must occur in matched pairs. The dipoles and loops are sensitive to the polarizations of incident electromagnetic plane waves. The dipoles are sensitive to the incident electric field components and the loops to magnetic field components of the incident waves. We exploit the invariance properties among the dipole and loop outputs. We show how the ESPRIT algorithm may be used with an arbitrary array of orthogonal loops and orthogonal dipoles to compute both

Manuscript received May 14, 1992; revised September 18, 1992.

The author is with the Department of Electrical Engineering, University of Kentucky, Lexington, KY 40506.

IEEE Log Number 9207126.